



Energy self-sufficient desalination stack as a potential fresh water supply on small islands



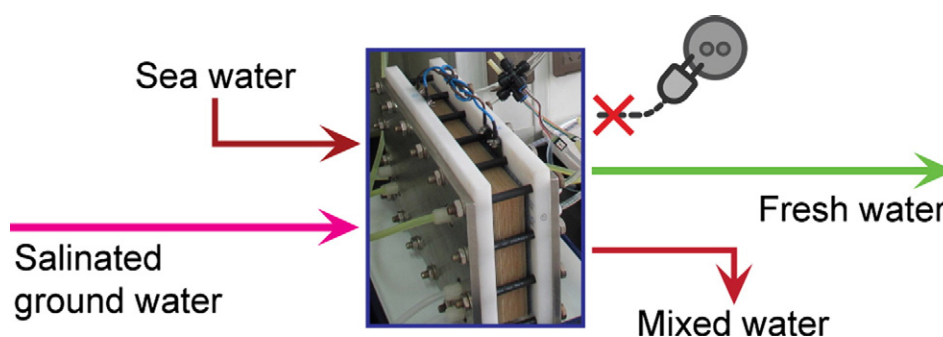
Qing Chen, Yuan-Yuan Liu, Chang Xue, Yu-Ling Yang, Wei-Ming Zhang*

College of Chemistry & Materials Engineering, Wenzhou University, Wenzhou 325000, PR China

HIGHLIGHTS

- An energy self-sufficient system was built to desalt brackish water on islands.
- Reverse electro dialysis and electro dialysis were integrated in single module.
- Salinity gradient energy was harvested for desalination.
- The system was well optimized for best overall performance.

GRAPHICAL ABSTRACT



ARTICLE INFO

Article history:

Received 19 October 2014
Received in revised form 9 December 2014
Accepted 10 December 2014
Available online 29 December 2014

Keywords:

Desalination
Energy self-sufficient
Reverse electro dialysis
Electro dialysis
Sea water intrusion

ABSTRACT

Sea water intrusion causes fresh water shortage on small islands, and desalination systems are needed to desalt the salinated water (brackish water) and produce fresh water. Unfortunately conventional desalination technologies can only work properly with stable external power inputs, which are usually not accessible in these rural areas. In this study we propose an integrated self-desalination stack that consists of alternate anion and cation ion exchange membranes and couples the technologies of reverse electro dialysis and electro dialysis. The salinity gradient energy between sea water and brackish water is harvested to demineralize another portion of brackish water directly in the same stack. The overall process is spontaneous and energy self-sufficient with minimum peripheral devices, and it is promising to provide fresh water supply especially for these rural residents on small islands.

© 2014 Elsevier B.V. All rights reserved.

1. Introduction

Potable fresh water (FW) is of vital importance for residents on small islands. There are about 1000 populated small islands in Pacific Ocean, and many islanders especially in rural areas are facing the challenge of FW shortage [1–3]. Groundwater is the main source of FW on many of these islands, which exists in the form of FW lenses, namely thin veneers of FW overlying sea water (SW) in highly permeated aquifers

[1]. These lenses are very limited and vulnerable because of the mixing and intrusion of SW [1–6]. The boundary between FW and SW is not sharp, and it occurs as a wide transition zone, where the salinity increases as the depth increases. The water in this transition zone is classified as brackish water (BW) [7].

It's widely believed that the first refugees of climate change will come from these islands [2]. The rising seawater levels and abnormal rainfall patterns will further ruin the FW lenses by SW intrusion [1,3]. The maximum salinity of FW is 400–500 mg/L NaCl according to the drinking water guidelines from World Health Organization (WHO) [8]. When salinity exceeds 500 mg/L NaCl, the water will be not drinkable,

* Corresponding author.

E-mail address: weiming@iccas.ac.cn (W.-M. Zhang).

and FW shortage happens. Desalination technologies are the key to resolve this issue [9–11]. Currently available processes such as multi-stage flash (MSF) distillation, multiple-effect distillation (MED), vapor compression (VC) distillation, reverse osmosis (RO) and electro-dialysis (ED) are well proven approaches to obtain FW from the SW or BW. Unfortunately the above desalination processes rely on stable power or heat source and economically effective only in large scale plants, while the majority of islanders (~80% in the 14 Pacific Island Countries) are living in rural areas [3] where the power grid is not available. Furthermore, there is no water distribution system in these areas, so distributed desalination systems are supposed to be close to the end-point household users. Desalination systems integrated with renewable energy technologies such as geothermal, solar or wind [12–14] are more suitable for these islanders, while the energy conversions in these systems are complex and costly. Electricity (as electronic current) must be obtained first and then used for the desalination later, and extra energy storage systems are usually needed to get stable electrical power [15].

According to the local geohydrology conditions, salinity gradient power is a reliable candidate of renewable energy source on these islands [16,17]. SW and BW are always available there, and they mix all the time underground. Reverse electro-dialysis (RED) is able to capture this salinity gradient energy as electricity [16,18–23], and theoretically it may provide the energy to meet the needs on these islands. However, RED is not an economic power generator at present because of the limited net power density, and further developments are needed [16,24,25]. Here in this study, we propose a novel architecture of energy self-sufficient desalination stack, in which RED and ED parts are coupled in single module. The ionic current generated in RED portion is the very driving force for ED desalination process, which is able to drive desalination directly and seamlessly within the stack, without any conversion. When compared with other desalination systems integrated with renewable energy technologies, the energy conversion practices reduce remarkably in this integrated stack. The produced FW has much more value than the small amount of energy which can be produced by current RED system alone on these small islands. In contrast with previous works based on the combination of RED and ED [26–30], the stack design in this work is much more applicable on these small islands. The integrated stack here ensures very low hydraulic pumping losses. Only after manually elevating 10 cm to help the feed water flow through the stack naturally, the FW will be produced constantly without any other external energy input. This feature is especially valuable for approaching the final energy self-sufficient goal, because it has the potential to get rid of all energized pumps in the whole system. The self-desalination stack in this study is promising to fill the gap for desalination need in these areas, which is helpful to relieve the FW shortage there.

2. Materials and methods

Fig. 1 presents a design of the self-desalination stack in our lab. There are four independent flow channels (CH1–4, also shown in Fig. S1A) in the integrated stack regulated by special designed spacers and membranes. The energy from salinity difference between BW (CH1) and SW (CH2) is harvested as ionic current in RED cell pairs, which is utilized for BW desalting in ED cell pairs to get FW (CH4) directly. The salinity gradient drives the ion migration needed for desalination in the stack, because the RED and ED subsystems are ionically connected. The electrodes and the short-circuit cable provide a closed loop for the current in the stack. The overall process is spontaneous and no external energy is needed.

Three different ion exchange membranes were used in this work, which were DF-120 anion exchange membranes (AEMs), DF-120 cation exchange membranes (CEMs) and Seleminion CMD CEMs. The Seleminion CMD CEMs were purchased from Asahi Glass Engineering Co., Ltd. Japan, and other membranes were purchased from Shandong Tianwei

Membrane Technology Co., Ltd. China. The main parameters of these membranes are listed in Table S1 in supplementary materials.

The spacers in this study were designed and manufactured in our lab, which had been described in our previous works [31,32]. This kind of spacer has a dimension of 260 mm (length) \times 130 mm (width) \times 0.9 mm (thickness). The spacer consists of polyethylene (PE) sheet and polypropylene (PP) turbulence accelerating mesh net, with tortuous flow path geometry of 33 mm (width) \times 567 mm (length), i.e. 187 cm² of effective area. The total flow rates (mL/min) and the flow velocities (cm/s) in stack can be readily converted from geometry of the flow paths. The PP mesh net has a porosity of 72%, and projected shadow effective area of the spacer is 135 cm². The specially designed pattern of the spacer enables 4 different flow channels at most, which is shown in Fig. S1.

RED and ED stacks with 2-compartment configurations, and integrated RED-ED stack with 4-compartment configuration, are assembled (shown in Fig. 1) independently. In this study, electrode membranes (CEMs near the electrodes) are Seleminion CMD CEMs, and all other membranes are DF-120 CEMs and AEMs respectively. Heavy Seleminion CMD CEMs are positioned adjacent to the electrodes, and they completely separate the electrode rinse from other feed streams to avoid potential contaminations. In addition, these heavy CEMs are durable for chemical contaminations, which is essential for the membrane adjacent to an electrode compartment [32]. The well designed components of the stack ensure good performance and no leakage.

Dimension stable electrodes (DSEs, from Suzhou Borui Industrial Material Science & Technology Co., Ltd. China, titanium electrodes with RuO₂–IrO₂ coatings) were used as electrodes in all stack designs in this study. Two different solutions were evaluated as electrode electrolytes. The first is 0.50 mol/L NaCl solution, and the other is mixture of 0.05 mol/L Na₄Fe(CN)₆ (sodium ferrocyanide), 0.05 mol/L K₃Fe(CN)₆ (potassium ferricyanide) and 0.25 mol/L NaCl [22,33]. All chemicals were of AR grade and purchased from Sinopharm Chemical Reagent Co., Ltd., China. The Na₄Fe(CN)₆ and K₃Fe(CN)₆ used here are completely nontoxic, and the health hazard ratings are the same as NaCl (rating 1 in NFPA 704). A miniature cell (shown in Fig. S2A) was built to evaluate the voltage loss in real stack. The key parameters, including electrode materials, heavy CEM, electrode rinse flow velocity and spacer thickness, are identical with real stacks. We applied constant current mode and recorded the voltage between electrodes.

Electrical conductivity distributions of the groundwater indicate the degree of SW intrusion on small islands. The salinities of the groundwater in many areas are as high as 1000 mg/L NaCl (1990 μ S/cm, see Fig. S3) even on wide islands such as Tongatapu [1], which makes the water significantly unpalatable. The situations on smaller islands are worse and many of them are uninhabited. To evaluate the performance of the above integrated RED-ED stack, we used 1000 mg/L NaCl solution as BW and 30,000 mg/L NaCl solution as SW feed streams in all experiments.

A Keithley 2400 source measure unit (SMU) was used in this study. With the ability of 4-quadrant operation, it was used here as a power source (for ED testing) as well as a sink (electronic load, for RED testing). 4-Wire configurations were involved in all tests to eliminate voltage loss in wires. A home-made console program was designed on a host computer to fully control the SMU via RS232 interface, which was similar to our previous works [34]. LEAD-2 (4 channels, 0–420 mL/min each) and BT-100 (2 channels, 0–48 mL/min each) metering pumps were used in this study, which were purchased from Baoding Longer Precision Pump Co., Ltd., China. The pumps were controlled by our home-made console program via digital TTL and 0–5 V analog signals. The concentrations of NaCl solutions are calculated from their conductivities according to the calibration curve shown in Fig. S3 in this work.

The change in Gibbs free energy of mixing is chosen to describe the energetics in both mixing and desalting processes. For NaCl solutions with relatively low concentrations, the maximum energy obtained by

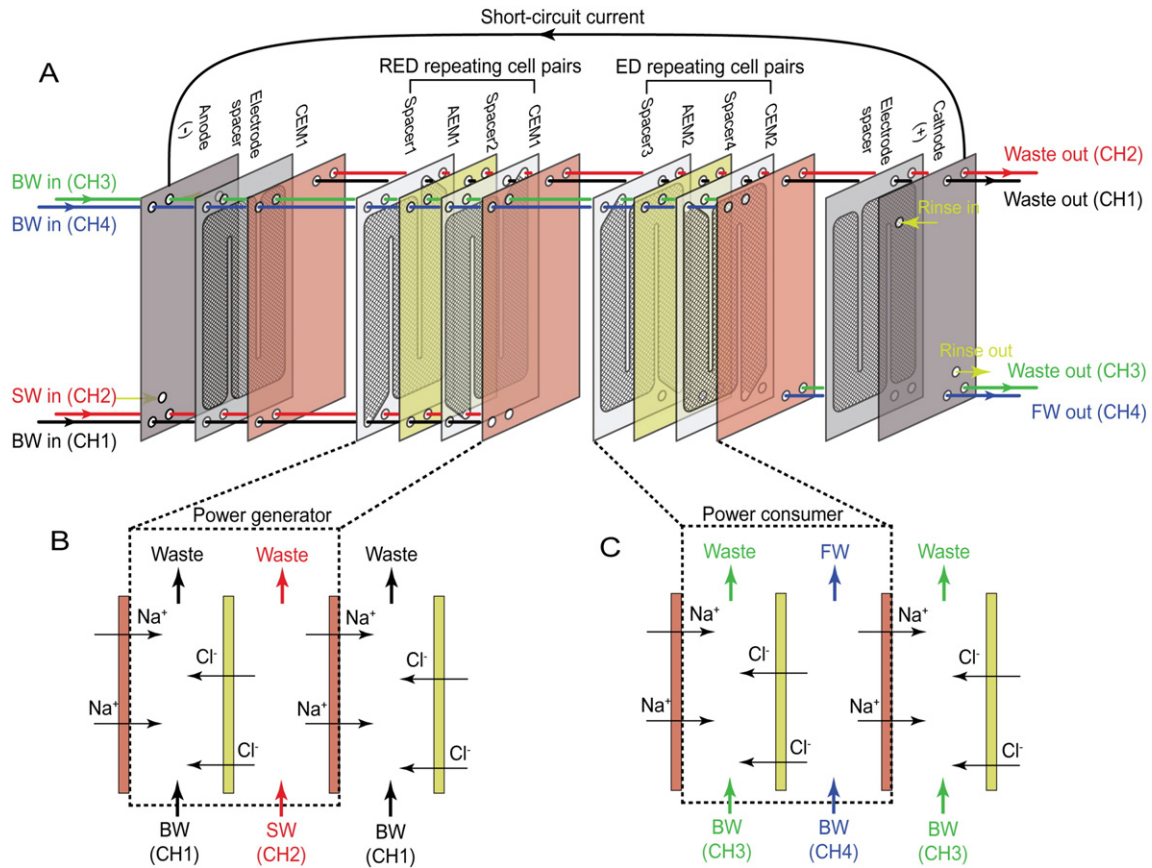


Fig. 1. Scheme of the integrated RED-ED stack (A), detailed ionic flow in RED (B) and ED (C) cell pairs. SW and BW flow through the stack with alternative cation exchange membranes (CEMs) and anion exchange membranes (AEMs). RED cell pairs work as a power generator and ED cell pairs work as a power consumer in series. The ionic current converts to electronic current on electrode surfaces, providing a closed loop for the current.

mixing BW and SW and the minimum energy required for desalting BW can both be calculated readily by the following formula: [35]

$$\frac{\Delta G_{mix}}{2RT} = \sum V_{out} c_{out} \ln(\gamma_{\pm, out} c_{out}) - \sum V_{in} c_{in} \ln(\gamma_{\pm, in} c_{in}) \quad (1)$$

where ΔG_{mix} is the change in Gibbs free energy of mixing, R is the gas constant, and T is the temperature. V , c and γ_{\pm} are the volume, molar concentration, and the average activity coefficient of a specific NaCl stream, respectively. The subscripts *out* and *in* represent the outlet and inlet streams for a specific process, respectively.

3. Results and discussion

3.1. Optimization of integrated RED-ED stack

The experimental data of the voltage consumptions on electrodes are plotted in Fig. S2B. The voltage loss in hexacyanoferrate solution is much lower than that in NaCl solution. The total voltage consumption is only ~40 mV at current density of 1 mA/cm² in hexacyanoferrate solution with CEMs, so hexacyanoferrate solutions were chosen as electrode rinses in all experiments to minimize the voltage consumption.

Generally speaking, there is considerable hydraulic loss in the flow channel of the stack. A digital differential pressure meter (DMP-2C, 0 to ± 10 kPa range, from Nanjing Nanda Wanhe Science and Technology Co., Ltd. China) was employed to monitor the pressure drops of the stack at various flow velocities, and the experimental data are plotted in Fig. 2A. The pressure drops in our stack are

much less than other designs [33], which benefits from thicker spacers. Thin flow spacers (such as 0.2–0.4 mm) do reduce overall electric resistance of the stack (2.93 Ω with 0.9 mm spacer and

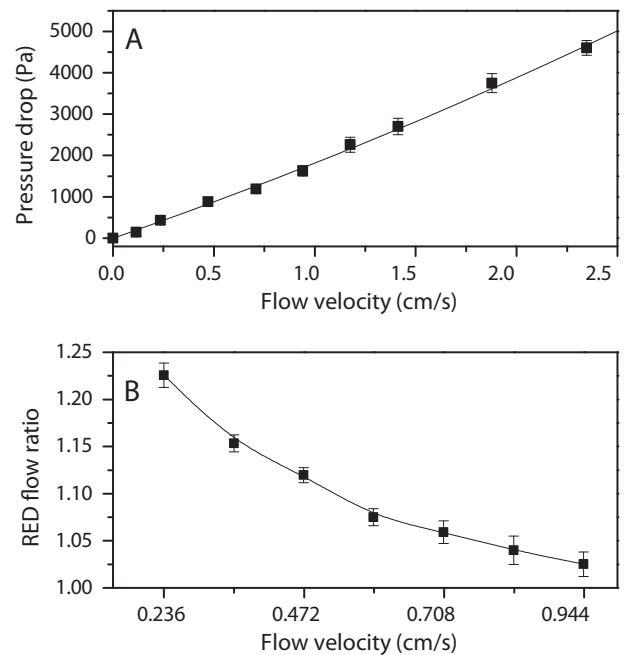


Fig. 2. (A) Water pressure drops at different flow velocities in the stack. (B) Osmotic water transport in the RED stack. The flow ratio here is defined as quotient of outlet flow rate of SW and BW. Data presented here are average of 4 independent runs.

0.98 Ω with 0.2 mm for 10 cell-pair RED stack), while the pressure drop will increase dramatically. The pressure drop is less than 4000 Pa (0.4 m water head loss) at 2 cm/s (356 mL/min for each stream in 10 cell-pair stack) flow velocity in our stack, which is just one-twelfth of that in previous works [33] with similar flow channel length. The low hydraulic loss is very helpful for the elimination of pumps in this work.

Tianwei DF-120 CEMs and AEMs were used in this study because of their low electric resistance. High water uptake and small thickness of these membranes are helpful to reduce the electric resistance, while the water permeation significantly increases. Water permeation across the membranes, also known as cross leakage, will cause contamination and performance degradation of the stack. The manufacturer of DF-120 membranes had not given the parameter on water permeation, so an experimental setup (shown in Fig. S4) was built to evaluate it. The average permeability of water is $15.2 \pm 0.5 \text{ cm} \cdot \text{h}^{-1} \cdot \text{bar}^{-1}$; this value is relatively high and may be worsened by leakage near the manifolds (the holes on the spacers and membranes). Special experiment considerations were involved to minimize the cross leakage in this study, including co-current flows, identical flow velocities and identical absolute pressure at the outlets.

A RED stack was assembled individually (composed of 10 RED cell pairs but no ED cell pair, as shown in Fig. 1) to better understand the output characteristics of the power generator part of the integrated stack. When BW and SW flow through the RED stack, water transfers across the membrane from BW channels (CH1) to SW channels (CH2). This phenomenon is caused by osmosis. The osmotic water transport at different flow velocities in the stack is shown in Fig. 2B. The flow ratio here is defined as the quotient of outlet flow rate of SW and BW. Since the concentration differences in the RED stack are basically constant, the osmotic water transport is more significant at low flow velocities for a longer contact time. A Keithley 2400 SMU was employed as programmable power sink. The flow velocity in stack was controlled by the metering pump; meanwhile the discharging current of the RED stack was modulated and corresponding stack voltage was recorded. Short-circuit current of the stack was also recorded. All above

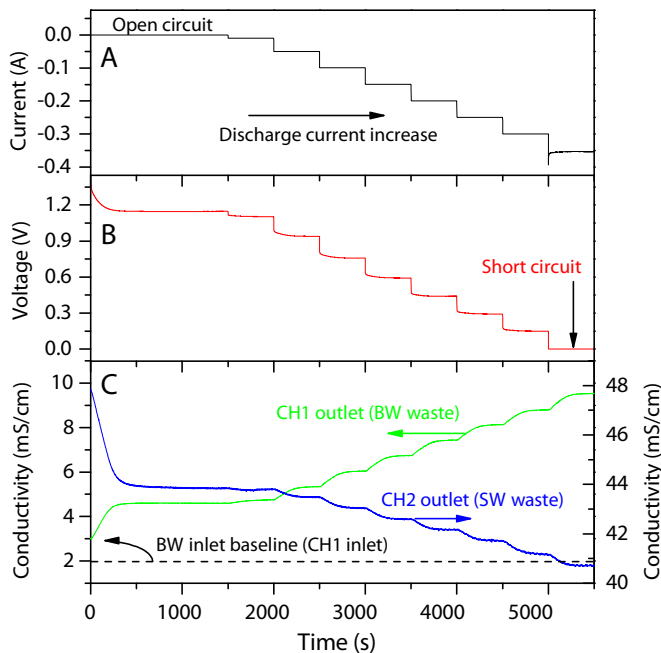


Fig. 3. Typical RED experimental data at flow velocity of 0.236 cm/s. (A) Discharge current of the RED stack; (B) corresponding stack voltage output; (C) corresponding conductivity profiles of the outlets. The RED stack was flushed with the feed streams at a high velocity (-2.36 cm/s) for 1 min before the test, which caused the high stack voltage as well as the rapid variations of the outlet conductivities at the initial stage.

operations were accomplished automatically by a home-made computer program. A typical RED experimental data are plotted in Fig. 3. The output voltage of the stack drops as the discharge current increases. The salinity in BW channel (CH1 in Fig. 1) increases in open-circuit mode, which indicates the existence of cross leakage. The BW salinity further increases as the discharge current goes up, which accords well with the ionic flow in Fig. 1B. The electrical characteristics of the RED stack at various discharge current densities as well as at different flow velocities were also evaluated automatically, and the results are presented in Fig. 4. Since higher salinity gradient would be retained at high flow velocity in stack, it's favored for higher stack voltage and power output. 130 mW net power output is achieved in our 10 cell-pair RED stack, namely 0.695 W/m^2 , which is comparable with state-of-art works [33].

An ED stack was also assembled (composed of 10 ED cell pairs but no RED cell pair in Fig. 1) to evaluate power consumption characteristics of the ED cell pairs. Both of the dilute and concentrate streams were BW (NaCl 1000 mg/L). Since the concentration difference is quite small, the osmotic water transport is negligible. Mixture of $\text{Na}_4\text{Fe}(\text{CN})_6$, $\text{K}_3\text{Fe}(\text{CN})_6$ and NaCl was also chosen as electrode rinse. Because the voltage consumption for electrode reaction is quite small ($\sim 0.04 \text{ V}$ for 1 mA/cm^2 , i.e. 187 mA for the stack, shown in Fig. S2B), it is reasonable to neglect this voltage consumption in our 10 cell-pair ED stack. The steady-state stack currents and salinities of the desalinated product water at different flow velocities are recorded in Table 1. The current efficiencies can be calculated readily by these results, which are 90–95% for all tests. BW as a concentrate stream here is very helpful to maintain the high efficiencies, because the total amount of NaCl migration for cross leakage will be much less than SW as concentrate stream.

The configurations of the integrated stack as well as the operation parameters such as flow velocity are optimized to achieve the best

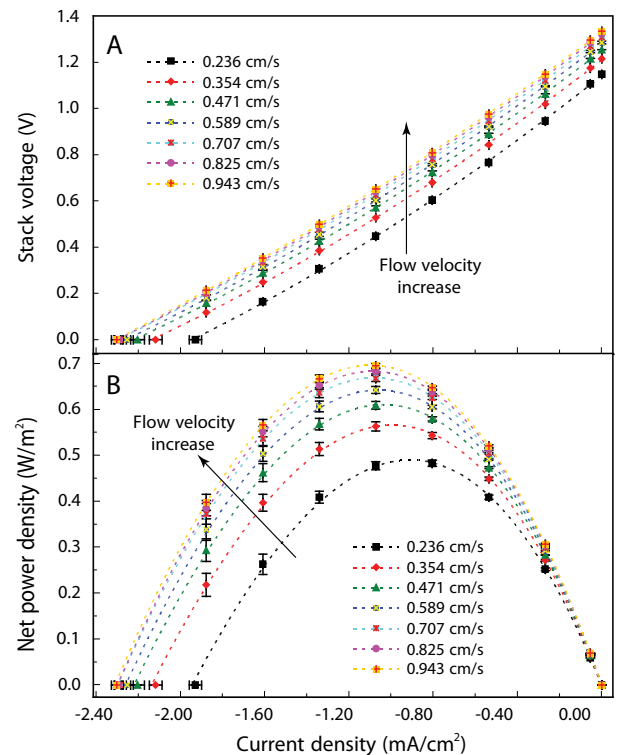


Fig. 4. Electric output characteristics of the 10 cell-pair RED stack. The fitted results of the experimental data are plotted with dashed curves. (A) Stack voltage output vs. discharge current density profiles at different feed velocities; (B) stack net power density output vs. discharge current density profiles. The current density is calculated from 187 cm^2 effective area. The power density output is normalized by total effective area of membrane pairs. Data presented here are average of 4 independent runs, and the error bars indicate the standard deviations.

Table 1

Performance evaluation results of ED stack at different feed flow velocities as well as different electric field strength. The current data were recorded by a SMU and the TDS data were calculated by the corresponding conductivities.

ED stack current (mA)	Flow velocity in stack (cm/s)							
ED product TDS (mg/L)	0.236	0.354	0.471	0.589	0.707	0.825	0.943	
Voltage drop (V/cell pair)	-0.10	-59	-71	-79	-84	-86	-88	-90
		498	603	677	736	784	810	832
-0.15	-77	-97	-111	-120	-126	-130	-133	
		319	440	529	609	672	715	746
-0.20	-85	-115	-137	-152	-161	-167	-173	
		236	324	414	498	572	624	661
-0.25	-88	-125	-155	-178	-192	-200	-209	
		210	257	324	403	482	545	587
-0.25	-90	-129	-166	-197	-217	-229	-241	
		199	230	272	335	408	471	519
-0.35	-92	-132	-172	-209	-236	-252	-268	
		189	220	251	288	345	414	461
-0.40	-93	-143	-175	-217	-251	-265	-292	
		184	210	236	262	304	382	414

overall system performance, which is based on the evaluation results of the above RED and ED stacks. There are two basic key rules during the optimization. First, total dissolved solids (TDSs) of the produced FW must be below the threshold of WHO drinking water guidelines, which is 450 mg/L NaCl. Second, the overall cost of the produced FW should be minimized. According to the fitting results of RED voltage outputs in Fig. 4A and the ED evaluation results in Table 1, optimization can be accomplished, and the detailed procedure is attached as Worksheet S1. The results indicate that the best electric field strength is 0.20 V per cell pair in ED stack, and the optimized flow velocity is 0.471 cm/s. The corresponding stack current is 137 mA (i.e. 0.73 mA/cm²), and the produced FW is 414 mg/L NaCl (0.85 mS/cm). To achieve such electric field strength and current density, it takes 2.6 RED cell pairs to drive 1 ED cell pair.

3.2. Lab test of integrated RED-ED stack

An integrated RED-ED stack with 11 RED cell pairs and 4 ED cell pairs (2.75:1) was assembled according to the above optimization results. A SMU and a cable were used to open and short the stack. The performance evaluation results of the integrated stack are presented in Fig. 5. The open-circuit voltage is 1.30 V and the short-circuit current is -153 mA (0.82 mA/cm², shown in Fig. 5A), which accords well with our modeling. When the stack is an open circuit, the conductivity

of ED product (CH4 outlet) is 1.99 mS/cm (1000 mg/L, same as feed BW, shown in Fig. 5B), indicating that there is no obvious salt leakage into this stream. Meanwhile the conductivity of ED concentrate (CH3 outlet) is significantly higher (2.40 mS/cm, shown in Fig. 5B) than feed BW, indicating significant salt leakage into this stream. Though cross-leakage always occurs in the stack, the CH4 channels are not adjacent to any SW channels (CH2) with high TDS, therefore the salt leakage in CH4 channels is not observed. One CH3 channel (the one next to the RED cell pairs) is adjacent to SW, so the salt leakage is obvious in the outlet stream. For the RED part, the situation is different. All RED dilute channels (CH1) are adjacent to SW (RED concentrate, CH2 channels), so the salt leakage is much more serious (4.30 mS/cm at outlet vs. 1.99 mS/cm at inlet, shown in Fig. 5B) in these channels. Since there is no obvious salt leakage into the ED product (CH4) stream, the current efficiency of ED desalination process remains high. When the stack is short circuit, ionic current flows as shown in Fig. 1B and C. The TDS of produced FW is 408 mg/L (0.84 mS/cm), which also accords well with our modeling. The working scenes of steady-state running system short circuited by SMU and cable are shown as Movie S1.

The material balance of the self-desalination process is shown in Fig. 5C. The TDSs of all outlet streams are calculated from the corresponding conductivities (except that of the RED SW outlet, TDS is estimated by NaCl mass balance, which also accords well with the conductivity data), and the flow rates are corrected by the osmotic water transport results in RED (Fig. 2B) and ED tests. There are 4 independent channels for both inlet and outlet streams. The overall ΔG_{mix} is -63.8 kJ/day according to Eq. (1), which indicates that the self-desalination process here is totally spontaneous. There is significant salt leakage from RED SW stream (CH2) to the adjacent ED concentrate stream (CH3) in this stack because of the large concentration gradient, so the RED and ED sub-processes are not isolated in this stack and the change in Gibbs free energies of mixing are unable to be calculated separately. It can be found that the total salt amount in ED outlet streams is higher than that of inlet streams in Fig. 5C.

Fortunately there is only one CEM (the one separating the RED part and the ED part in Fig. 1A) that is bothered by this inter-stack leakage issue, and the portion of such leakage will abate as the stack scales up. The mass balance for RED-ED stack with much more cell pairs (scaled up proportionally) will be different from Fig. 5C. The salinity will be 1592 mg/L for the ED concentrate (CH3 outlet) and 26,777 mg/L for RED SW (CH2 outlet). In this situation, the RED and ED processes in the stack are virtually independent. The ΔG_{mix} for the RED and ED sub-processes is -62.1 kJ/day and 1.44 kJ/day respectively, and the overall ΔG_{mix} is -60.7 kJ/day (the detailed calculation process is

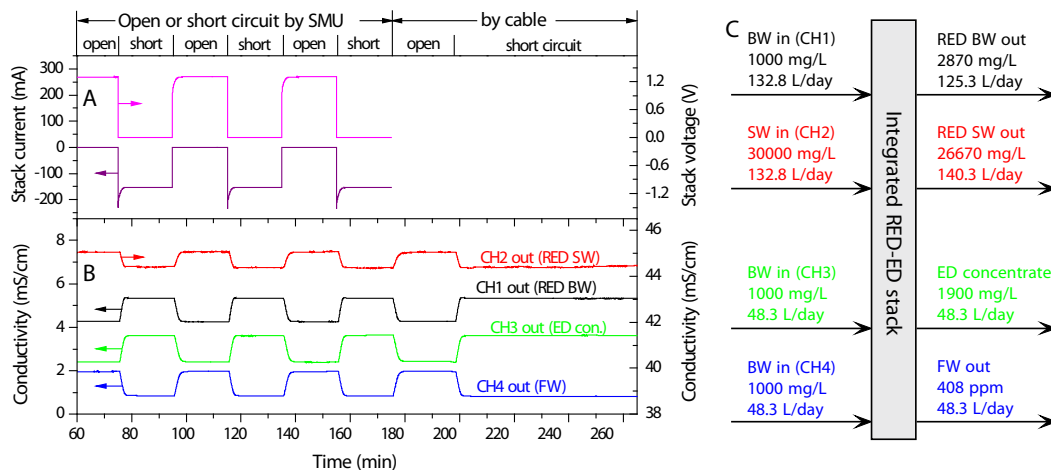


Fig. 5. Performance evaluation of the integrated RED-ED stack. (A) Open-circuit voltage and short-circuit current profile recorded by the SMU. (B) Conductivity profiles of all outlets during the open-short switches. (C) The experimental material balance of process in the short-circuit RED-ED stack.

shown in Worksheet S2). The overall thermodynamical energy efficiency is relatively low (2.3%) in the integrated stack. As shown in Fig. 4B, the electric power output is 108 mW (0.58 W/m²) for the 10 cell-pair RED stack at 0.471 cm/s flow velocity and 150 mA (0.80 mA/cm²) discharge current, namely 119 mW (10.3 kJ/day) output for the 11 cell-pair RED in the integrated stack at equivalent operational parameters. The RED part obtains 16.5% energy as electric power (10.3 kJ/day) from the free energy of mixing (−62.1 kJ/day). The nonideal characteristics of the RED stack, such as co-ion leakage on the membranes and cross-leakage in the stack, cause a great loss of the free energy. Furthermore, the high electric resistances of the RED stack (ascribed to high electric resistances of BW streams as well as the membranes) wastes considerable energy. The 16.5% thermodynamical energy efficiency is reasonable for the current RED process. The current efficiency of ED sub-process is pretty high, which is 91%. The ED sub-process consumes all the output power from RED (10.3 kJ/day), while the minimum energy required for ED desalting process is 1.44 kJ/day, so the thermodynamical energy efficiency of ED sub-process is 14.0%. To maintain a reasonable current density in ED stack, extra power is needed to overcome the high electric resistance of ED stack and the energy efficiency is lowered, especially for low feed TDS situations. The thermodynamical energy efficiency of the overall process is the product of that in RED and ED sub-processes, which is 2.3%. Although the efficiency is not high (limited by the restrictions of practical RED and ED engineering in this study), it is still good enough to produce a stable FW supply (as shown in Fig. 5C).

3.3. Minimum self-desalination system without pumps

Our stack design ensures much lower hydraulic resistance. The pressure drop in stack is only 850 Pa (8.5 cm water head loss, shown in Fig. 2A) at the optimized flow velocity of 0.471 cm/s. So the feed solutions are able to flow through the stack naturally if appropriate water head is maintained. Our experiments indicate that a 10 cm water head is suitable to maintain a 0.47 cm/s flow velocity, and the extra water head is lost in the pipes. The most common ground water supply on low-lying islands is hand-dug wells. The salinated ground water (i.e. BW) is abstracted by buckets and hand pumps [1]. SW is even more abundant in these areas. A 10 cm water head is easy to obtain manually during the water abstraction. After the BW and SW feed solutions elevated, this system can spontaneously produce FW without any pumps. The working scenes of this minimum self-desalination system are shown in Movie S2. The electrode rinses flow through the integrated stacks in a rocking-chair manner and no consumption is observed. TDS of the produced FW is 420 mg/L NaCl (0.86 mS/cm), and that is nearly the same as lab test results with pumps. The overall process is totally spontaneous with minimum peripheral devices, and the total material cost of the system is as low as \$200, which only consists of the stack and corresponding containers. This system produces 48.3 l of FW water (~420 mg/L) daily, consuming 229.4 l of BW and 132.8 l of SW. The system capacity is adequate for most ordinary household users. The BW recovery is 21% and the salt rejection is 58%. The waste BW streams (CH1 and CH3, 173.6 l per day in total) are still suitable for other household needs such as bathing and washing. The system lifespan is expected to be long if bio-fouling is well controlled, and the fresh water cost (capital only) is \$7.0/m³ base on 2-year lifespan estimation. Furthermore, there is no brine disposal problem in this process, since no effluents with higher salinity than SW are generated.

Unlike traditional ED or RED stacks, the electrode system in this integrated RED-ED stack only provides a closed loop for the current. It's possible to eliminate the electrode system completely by providing an ionic current loop. In Fig. 1A, the Na⁺ migrates out of the anode chamber and into the cathode chamber, and an ionic current loop can be achieved if an ion conductive pathway is provided to connect these two chambers. In this situation special electrode rinses such as hexacyanoferrate solution are not needed any more. Further work is

in progress in our lab to design an electrode-free stack, which is very promising to reduce the system cost and improve the overall performance. The biofouling issue of the membrane is the key risk for achieving long-term system stability, which must be mitigated before actual applications. Abatement plans for conventional RED systems should also work for this system.

4. Conclusions

The 1000 populated small islands in Pacific Ocean are home to over 9 million people, and many of them face the challenge of obtaining safe drinking water, constrained by their remoteness, small size, natural vulnerability, and limited financial resources. We design and construct a novel energy self-sufficient stack to obtain FW directly from BW and SW, in which RED and ED are coupled in a single module. The energy from salinity difference between SW and BW is harvested in the RED cell pairs, and it drives the desalting process in ED cell pairs. The stack configurations and corresponding operational parameters are carefully optimized to achieve best overall system performance. After elevating the BW and SW a little (~10 cm) manually, the feed streams are able to flow through the stack naturally. The overall process is spontaneous and no extra external energy is needed. This self-desalination stack relies on minimum peripheral devices, and the total cost is low. The system cost is \$200, and the cost of fresh water produced is about \$7.0/m³ base on 2-year system lifespan. This desalination process is totally environment-friendly without brine disposal problem and greenhouse gas emission. The overall system is much less complex than comparable desalination system integrated with other renewable energies, and the system footprint is smaller. The above features enable this self-desalination system to be a potential solution to quench the thirsts of people during the duel between FW and SW on these vulnerable islands. In addition, recent researches indicate that vast offshore BW reserves sequestered during the last glacial period are common occurrences in coastal regions all around the world [36,37]. This self-desalination system may also be applied in these regions as a potential FW supply.

Acknowledgments

The authors are grateful for the financial support by the National Natural Science Foundation of China (Project Nos. 21203139 and 21003097).

Appendix A. Supplementary data

Table S1, Figures S1–S4, Microsoft excel worksheet S1–S2 and Movies S1–S2. This information is available free of charge via the Internet or from the authors. Supplementary data associated with this article can be found, in the online version, at <http://dx.doi.org/10.1016/j.desal.2014.12.010>.

References

- [1] I. White, T. Falkland, Management of freshwater lenses on small Pacific islands, *Hydrogeol. J.* 18 (1) (2010) 227–246.
- [2] Small Islands in the Pacific: Duel Between Freshwater and Seawater, <http://www.sciencedaily.com/releases/2010/12/101215102434.htm>.
- [3] D. Duncan, Freshwater Under Threat—Pacific Islands, United Nations Environment Programme (UNEP), Bangkok, 2011. 25.
- [4] J.V. Cruz, M.O. Silva, Groundwater salinization in Pico Island (Azores, Portugal): origin and mechanisms, *Environ. Geol.* 39 (10) (2000) 1181–1189.
- [5] H. Chen, Y. Zhang, X. Wang, Z. Ren, L. Li, Salt-water intrusion in the lower reaches of the Weihe River, Shandong Province, China, *Hydrogeol. J.* 5 (3) (1997) 82–88.
- [6] J.-C. Comte, O. Banton, J.-L. Join, G. Cabioch, Evaluation of effective groundwater recharge of freshwater lens in small islands by the combined modeling of geoelectrical data and water heads, *Water Resour. Res.* 46 (6) (2010) W06601.
- [7] R.S.K. Barnes, What, if anything, is a brackish-water fauna? *Trans. R. Soc. Edinb. Earth Sci.* 80 (3–4) (1989) 235–240.
- [8] World Health Organization (WHO), Guidelines for Drinking-water Quality, 4th ed. Gutenberg, Malta, 2011. 223.

- [9] O.K. Buros, *The ABCs of Desalting*, 2nd ed. International Desalination Association, Topsfield, 2000.
- [10] M.A. Shannon, P.W. Bohn, M. Elimelech, J.G. Georgiadis, B.J. Marinas, A.M. Mayes, Science and technology for water purification in the coming decades, *Nature* 452 (7185) (2008) 301–310.
- [11] M. Elimelech, W.A. Phillip, The future of seawater desalination: energy, technology, and the environment, *Science* 333 (6043) (2011) 712–717.
- [12] E. Mathioulakis, V. Belessiotis, E. Delyannis, Desalination by using alternative energy: review and state-of-the-art, *Desalination* 203 (1–3) (2007) 346–365.
- [13] M.A. Eltawil, Z. Zhengming, L. Yuan, A review of renewable energy technologies integrated with desalination systems, *Renew. Sust. Energ. Rev.* 13 (9) (2009) 2245–2262.
- [14] A. Subramani, M. Badruzzaman, J. Oppenheimer, J.G. Jacangelo, Energy minimization strategies and renewable energy utilization for desalination: a review, *Water Res.* 45 (5) (2011) 1907–1920.
- [15] Z. Yang, J. Zhang, M.C.W. Kintner-Meyer, X. Lu, D. Choi, J.P. Lemmon, J. Liu, Electrochemical energy storage for green grid, *Chem. Rev.* 111 (5) (2011) 3577–3613.
- [16] B.E. Logan, M. Elimelech, Membrane-based processes for sustainable power generation using water, *Nature* 488 (7411) (2012) 313–319.
- [17] G.Z. Ramon, B.J. Feinberg, E.M.V. Hoek, Membrane-based production of salinity-gradient power, *Energy Environ. Sci.* 4 (11) (2011) 4423–4434.
- [18] R.E. Pattle, Production of electric power by mixing fresh and salt water in the hydroelectric pile, *Nature* 174 (1954) 660.
- [19] M. Turek, B. Bandura, Renewable energy by reverse electrodialysis, *Desalination* 205 (1–3) (2007) 67–74.
- [20] J.W. Post, H.V.M. Hamelers, C.J.N. Buisman, Energy recovery from controlled mixing salt and fresh water with a reverse electrodialysis system, *Environ. Sci. Technol.* 42 (15) (2008) 5785–5790.
- [21] P. Długołęcki, A. Gambier, K. Nijmeijer, M. Wessling, Practical potential of reverse electrodialysis as process for sustainable energy generation, *Environ. Sci. Technol.* 43 (17) (2009) 6888–6894.
- [22] J. Veerman, R.M. de Jong, M. Saakes, S.J. Metz, G.J. Harmsen, Reverse electrodialysis: comparison of six commercial membrane pairs on the thermodynamic efficiency and power density, *J. Membr. Sci.* 343 (1–2) (2009) 7–15.
- [23] D.A. Vermaas, S. Bajracharya, B.B. Sales, M. Saakes, B. Hamelers, K. Nijmeijer, Clean energy generation using capacitive electrodes in reverse electrodialysis, *Energy Environ. Sci.* 6 (2) (2013) 643–651.
- [24] Y. Kim, B.E. Logan, Hydrogen production from inexhaustible supplies of fresh and salt water using microbial reverse-electrodialysis electrolysis cells, *Proc. Natl. Acad. Sci. U. S. A.* 108 (39) (2011) 16176–16181.
- [25] R.D. Cusick, Y. Kim, B.E. Logan, Energy capture from thermolytic solutions in microbial reverse-electrodialysis cells, *Science* 335 (2012) 1474–1477.
- [26] G.W. Murphy, Osmionic demineralization, *Ind. Eng. Chem.* 50 (8) (1958) 1181–1188.
- [27] R.E. Lacey, *Development, Construction, and Testing of Osmionic Demineralizers*, University of Michigan Library, 1960.
- [28] G.W. Murphy, R.R. Matthews, Migration in transference cells with and without membranes—application to osmionic demineralization, *Electrochim. Acta* 12 (8) (1967) 983–998.
- [29] J. Veerman, Rijnwater ontzouten hoeft geen energie te kosten, *Polytech. Tijdschr.* (1994) 52–55.
- [30] Sparrow, B. S., Zoshi, J. A., Tang, J. H. B. Method for desalinating saltwater using concentration difference energy. U.S. Patent 8,236,158, Aug. 7, 2012.
- [31] W.-M. Zhang, J.-X. Zhuang, Q. Chen, S. Wang, W.-G. Song, L.-J. Wan, Cost-effective production of pure Al₁₃ from AlCl₃ by electrolysis, *Ind. Eng. Chem. Res.* 51 (34) (2012) 11201–11206.
- [32] J.-X. Zhuang, Q. Chen, S. Wang, W.-M. Zhang, W.-G. Song, L.-J. Wan, K.-S. Ma, C.-N. Zhang, Zero discharge process for foil industry waste acid reclamation: coupling of diffusion dialysis and electrodialysis with bipolar membranes, *J. Membr. Sci.* 432 (2013) 90–96.
- [33] J. Veerman, M. Saakes, S.J. Metz, G.J. Harmsen, Electrical power from sea and river water by reverse electrodialysis: a first step from the laboratory to a real power plant, *Environ. Sci. Technol.* 44 (23) (2010) 9207–9212.
- [34] W.-M. Zhang, J.-S. Hu, H.-T. Ding, L.-J. Wan, W.-G. Song, Programmed fabrication of bimetallic nanobarcodes for miniature multiplexing bioanalysis, *Anal. Chem.* 81 (7) (2009) 2815–2818.
- [35] N.Y. Yip, M. Elimelech, Thermodynamic and energy efficiency analysis of power generation from natural salinity gradients by pressure retarded osmosis, *Environ. Sci. Technol.* 46 (9) (2012) 5230–5239.
- [36] T. Bakken, F. Ruden, L. Mangset, Submarine groundwater: a new concept for the supply of drinking water, *Water Resour. Manage.* 26 (4) (2012) 1015–1026.
- [37] V.E.A. Post, J. Groen, H. Kooi, M. Person, S. Ge, W.M. Edmunds, Offshore fresh groundwater reserves as a global phenomenon, *Nature* 504 (7478) (2013) 71–78.